Application of the bond valence method to reverse Monte Carlo produced structural models of superionic glasses

Jan Swenson[1] and Stefan Adams[2]
[1]*Department of Applied Physics, Chalmers University of Technology, S-412 96 Göteborg, Sweden*
[2]*GZG, Abteilung Kristallographie, Universität Göttingen, Goldschmidtstraße 1, D-37077 Göttingen, Germany*
(Received 6 December 2000; revised manuscript received 2 April 2001; published 20 June 2001)

The reverse Monte Carlo RMC method has shown to be a useful tool for extracting structural properties from diffraction data of disordered systems, such as ion-conducting glasses. In this paper we investigate ion conduction in Ag-based superionic glasses by simple random-walk simulations based on the bond-valence information present in the RMC-produced structural models. Using this method we are able to explore the ion-conduction pathways and to calculate the ionic conductivity on a quantitative basis. The migration pathways are assumed to be the regions of the structural models where the valence mismatch for the mobile ion remains below a threshold value. The results for the AgI-doped glasses show that there are no long-range migration pathways for Ag sites in an entire iodine environment. Rather, the Ag^+ ions are generally moving between sites with a mixed oxygen-iodine coordination. The method is able to predict the ionic conductivity of highly AgI-doped superionic glasses, but tends to overestimate the conductivity of undoped glasses (with $\sigma < 10^{-5}\,\Omega^{-}\,\mathrm{cm}^{-1}$) and underestimate the conductivity of highly conducting crystalline α-AgI. The discrepancies for these materials are discussed, as well as the possibility and limitations of using a similar approach to study the frequency dependence of the conductivity.

DOI: 10.1103/PhysRevB.64.024204 PACS number(s): 66.10.Ed, 61.43.Fs

I. INTRODUCTION

Structural properties of glasses in general, and complicated multicomponent glasses in particular, are difficult to extract directly from experimental results. This is partly because global structural investigations by diffraction techniques are only providing a one-dimensional average representation of the structure, usually without any information of partial pair correlations for a single experiment. For simple glasses, the nearest-neighbor distances and coordination numbers have been determined predominantly by neutron or x-ray diffraction. However, even for relatively simple glasses, such as B_2O_3 and SiO_2, many controversies have continued through the years concerning the structure beyond the nearest neighbors. They concern, for example, the presence of few membered rings,[1,2] the origin of the first sharp diffraction peak in network glasses,[3–12] the degree of intermediate-range ordering,[6,10,12] and similarities to corresponding crystal structures.[3,4]

For more complicated multicomponent glasses, such as superionic glasses, the structure is even less known. It is then more difficult to extract structural information directly from diffraction experiments, especially when the use of isotope substitution to obtain elemental contrast is not possible. Instead, the knowledge originates often from atom or molecule specific probes such as nuclear magnetic resonance (NMR), extended x-ray-absorption fine-structure (EXAFS) and vibrational spectroscopy, which provide local information on a specific part of the structure. However, to get a relevant view of the total structure it is evident that some kind of structural modeling is needed for most multicomponent glasses. This can be done by conventional simulation techniques like molecular dynamics and ordinary Monte Carlo. The problem with these simulation techniques is, however, that they require interatomic model potentials between the particles, which are difficult to define for chemically complicated glasses. This often leads to problems in reproducing experimental data quantitatively. To master this problem and make direct use of the available experimental diffraction data it is appropriate to use the reverse Monte Carlo RMC modeling method.[13,14] The RMC method produces three-dimensional structural models in quantitative agreement with the measured data, although it should be noted that without using additional structural information it is unlikely that the method will produce sensible structural models.[15] Additional information, such as closest atom-atom approaches and coordination numbers, can be included in the structural models as physical constraints. Such constraints are normally based on other experimental results (e.g., NMR, Raman, or infrared-absorption data) or chemical knowledge and are often necessary to reduce the number of possibilities to fit the data with a physically unrealistic structure. For ordinary network glasses it is usually easy to build up a realistic network structure simply by including constraints on the connectivity between the network atoms (e.g., in the case of SiO_2, all Si are four coordinated to O and all O are two coordinated to Si). However, in the case of ionic glasses even the short-range structural knowledge is usually limited and it is more difficult to use precise coordination constraints.

To overcome this difficulty we have in this paper used a constraint based on bond-length distributions in related crystalline compounds.[16–18] During the past decades the bond-valence method proved to be a valuable tool in crystallography to check the plausibility of proposed crystal structures. It is based on the idea that the total bond-valence sum V of, e.g., a silver atom in any compound may be expressed as

$$V(\mathrm{Ag}) = \sum_X s_{\mathrm{Ag}\text{-}X}, \tag{1}$$

where the individual bond valences $s_{\text{Ag-}X}$ of bonds to all adjacent anions X are calculated from tabulated empirical bond-length bond-valence parameter sets (see, e.g., Refs. 19 and 20) of the type

$$s_{\text{Ag-}X} = \exp\left[\frac{R_0 - R_{\text{Ag-}X}}{b}\right]. \tag{2}$$

Equilibrium sites for a monovalent cation like Ag^+ are expected to exhibit a bond-valence sum close to $V_{\text{ideal}}=1$. For the sake of simplicity the established literature bond-valence parameter tables rely on the approximation that only the nearest-neighboring counterions contribute to the bond valence and that the parameter b may be treated as a universal constant. This turned out to be suitable for common applications, such as checking the plausibility of crystal-structure determinations or locating missing atoms in a structure.

The bond-valence approach can furthermore be used to determine migration pathways of mobile ions in solid electrolytes, since it is likely that the ion transport from one equilibrium site to another follows the energetically most favorable pathway with the lowest valence mismatch $\Delta V = |V_- V_{\text{ideal}}|$ along the way. As exemplified in Refs. 21 and 22, this special application requires the consideration of higher coordination shells as well as differences in the polarizability of the ions (which can be accomplished by the use of appropriate bond-valence parameters b).

The ionic transport in a variety of crystalline and a few glassy ion-conducting systems has been successfully investigated by this technique (see, e.g., Refs. 18 and 21–29). However, in order for the bond-valence method to work and give reasonable results it is important to have realistic structural models, particularly concerning the local environment of the mobile ions. This is usually not a great problem for crystalline conductors, where the structure is normally well known, but a major difficulty in the investigation of glassy conductors. In this paper we show how the local environment of the mobile Ag^+ ions can be improved by the inclusion of a soft bond-valence constraint in the RMC modeling of the Ag-based superionic glasses $(AgI)_x$-$(Ag_2O$-$yB_2O_3)_{1-x}$ ($x=0$, 0.6; $y=1$, 2, 4), $(AgI)_x$-$(AgPO_3)_{1-x}$ ($x=0-0.5$), and $(AgI)_{0.75}$-$(Ag_2MO_4)_{0.25}$ ($M=$Mo, W). The structural findings are compared with previous RMC results obtained without the inclusion of any bond-valence constraint.[30–33] We further show how the structural models and the bond-valence method can be used to elucidate the conduction pathways in ion-conducting glasses. The simulation of the Ag^+ transport in these glasses as a random walk within the bond-valence pathways not only permits a prediction of the dc conductivity from the structural model but also enables us to elucidate the nature of ion transport in glasses. The method provides a simple tool to investigate with a justifiable computational effort, e.g., the influence of different counterions on the long-range transport of mobile ions or other details of the trajectories that are difficult to identify experimentally from both structural studies and spectroscopic measurements.

II. THE BOND-VALENCE SUM PSEUDOPOTENTIAL METHOD

A. Conduction pathway models from bond-valence maps

For the comparatively clear case of crystalline α-AgI Garrett *et al.*[23] have demonstrated that migration pathways of mobile ions, as determined from crystallographic determinations of the anharmonic atomic displacement factors in this superionic conductor,[34] closely resemble the pathways of lowest bond-valence mismatch between the equilibrium Ag sites visualized in maps of the bond-valence mismatch.

Our three-dimensional bond-valence sum maps for the RMC-produced structural models [with volumes ranging from about 50 000–100 000 Å^3 for the different glasses] were generated by calculating the bond-valence sum for a hypothetical Ag^+ at all 161^3 grid points of a three-dimensional cubic primitive grid. At each position contributions from all anions up to a cutoff distance of 8 Å were considered. Grid points in the vicinity of other types of cations M^+ (i.e., at distances below the radii sum of Ag and M) are marked as inaccessible for the hypothetical Ag^+. Thereby we arbitrarily subdivide each structural model into a primitive array of about 4 000 000 cubic volume elements with edge lengths of 0.2–0.3 Å. The volume elements are classified as ''*accessible*'' for an Ag^+ if the Ag valence sum V at its center lies in the interval 1.00 ± 0.05 or if the valence mismatch $\Delta V = |V - V_{\text{ideal}}|$ changes its sign across the volume element. The second criterion is needed to cushion the influence of our limited grid resolution. The choice of the fixed valence mismatch threshold $\Delta V = 0.05$ valence units for all the systems was inspired by the observation that this equals the minimum valence mismatch for which bond-valence pathways in the crystal-structure model of α-AgI become infinite. Nevertheless this choice remains to some extent arbitrary.

Pathways for ion transport then correspond to clusters of adjacent ''accessible'' sites and the infinite cluster (which exists in all the investigated glasses for the chosen valence mismatch threshold) represents the continuous conduction pathway for the long-range ion transport giving rise to dc ionic conductivity. In previous papers[22] we have shown for a few glasses that the volume fraction F of the respective infinite pathway clusters is related to the experimental dc conductivity σ of the system at the temperature T of the experimental diffraction data used to build the RMC structure model. We found that

$$\log(\sigma T) \propto \sqrt[3]{F} \tag{3a}$$

and that the experimentally determined activation energy E_σ for ion migration is given by

$$\left(\frac{E_\sigma}{k_b T}\right) \propto \sqrt[3]{F}. \tag{3b}$$

Both relations also hold for the more comprehensive range of systems considered in this paper.

B. Random-walk simulations

In this work the bond-valence isosurfaces from RMC models are further examined by a simulation of Ag^+ motion through the systems as random hops from one of the above-mentioned volume elements to the next one. In each step of the simulation the direction of the attempted motion for each Ag^+ is chosen randomly among the 26 adjacent face, edge, or vertex sharing cubes. This ensures that a mobile ion may in principle pass any complex-shaped bottle neck of the bond-valence pathways. Successful hops require that the target cube in the randomly chosen direction is ''accessible'' according to the criteria defined in the previous section. This approach is slightly more sophisticated than a similar methodology that was previously used by Wicks *et al.*[31] for investigation of the conduction process in AgI-doped silver phosphate glasses. They used a hard-sphere Monte Carlo simulation method to move the mobile Ag^+ ions within the accessible free volume of the frozen glass network. However, using their approach the mobile Ag^+ ions are moving within all the accessible free volume, whereas in our model the Ag^+ ions are assumed to preferably move along the walls of the free volume.

Due to the small hop distance of about 0.2–0.3 Å an individual hop in the simulation rather represents thermal motion than actual jump processes by which the mobile ion would reach a different equilibrium site. For the room-temperature models the time a mobile Ag^+ would need to cross one of these elementary cubes with thermal velocity corresponds to roughly 10^{-13} s, i.e., the time steps of the model are of the order of magnitude of thermal vibration periods. In order to account for the difference in the hop length, a hop to one of the six face sharing cubes as well as any unsuccessful attempt is counted as one time step, while hops to one of the 12 edge sharing cubes are counted as $\sqrt{2}$ time steps and hops to one of the eight vertex sharing cubes as $\sqrt{3}$ time steps. It should be noted however that the probability that both the actual and the target site belong to the pathway decreases with the distance of the target site. Thus the success probability for hops to face sharing cubes is higher than for hops to the more distant vertex sharing sites. This will be addressed further below.

Such random walks were simulated using all the positions of ''mobile Ag^+'' as starting points, meaning all those Ag^+ positions of the underlying RMC structure model that are either located in ''accessible'' sites or can reach an ''accessible'' site within a single hop. As expected the fraction of these ''mobile'' Ag^+ ions increases with an increasing volume fraction F of the pathway from about 5% of all Ag^+ in Ag_2O-$4B_2O_3$ to approximately 20% for the glassy system $(AgI)_{0.75}$-$(Ag_2MO_4)_{0.25}$ (M=W, Mo) and to about 37% for the RMC models of crystalline α-AgI (see Fig. 1). All the remaining Ag^+ are strictly ''immobile'' in the frame of this approach.

It is quite clear from the beginning that such a simplified approach cannot reproduce the behavior of the mobile ions in the real system in every detail (e.g., interactions between the mobile ions as well as all motions of other types of ions are completely neglected). Therefore it has to be checked against experimentally known features of the ion transport in glasses, and under which circumstances and to which extent such simulations can yield physically sensible results. Questions that may be addressed by this approach include the prediction of diffusion constants from structural models as well as the contribution of differently coordinated ions of the mobile species to the long-range diffusion constant and details of the particle trajectories such as the occurrence of a correlated forward/backward hopping.

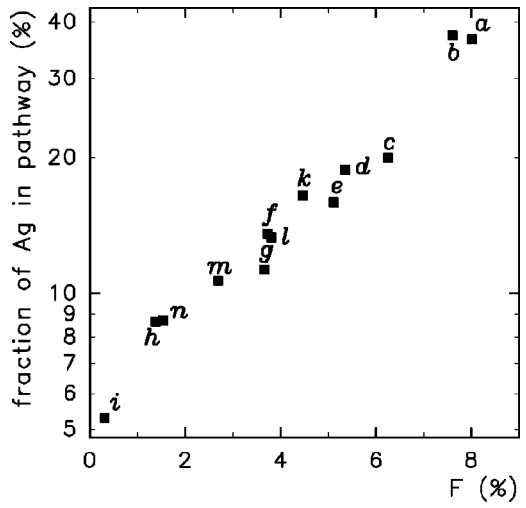

FIG. 1. Correlation between the fraction of all Ag that are ''mobile,'' i.e., located within any bond-valence pathway and the volume fraction F of the infinite pathways in RMC structure models of crystalline α-AgI at 740 K (a) and at 525 K (b) as well as glassy $(AgI)_{0.75}$-$(Ag_2WO_4)_{0.25}$ (c), $(AgI)_{0.75}$-$(Ag_2MoO_4)_{0.25}$ (d), $(AgI)_{0.6}$-$(AgO\text{-}B_2O_3)_{0.4}$ (e), $(AgI)_{0.6}$-$(Ag_2O\text{-}2B_2O_3)_{0.4}$ (two independent structure models *f, g*), Ag_2O-$2B_2O_3$ (h), Ag_2O-$4B_2O_3$ (i), $(AgI)_x(AgPO_3)$ with $x=0.5$ (k), 0.3 (l), 0.1 (m), and AgPO3 (n). All the glass structure models are based on room-temperature data.

III. THE RMC METHOD WITH A NEW BOND-VALENCE CONSTRAINT

The RMC modeling was based on both neutron- and x-ray-diffraction data, previously published in Refs. 30–33. The RMC method has been extensively described elsewhere,[13,14,35,36] so here we will only give a brief summary and some details of the particular constraints we have used in the simulations. The crucial difference between RMC and ordinary Monte Carlo simulations is that RMC employs experimental data instead of interatomic potentials in the minimizing procedure. RMC uses a standard Metropolis Monte Carlo algorithm[37] (Markov chain, periodic boundary conditions, etc.) but with the ''sum of squares'' difference between the measured structure factors and those calculated from the RMC configuration as the ''driving parameter'' in place of the energy. Data from different sources (neutron, x rays, and EXAFS) may be combined. In this way, the RMC method produces three-dimensional models of the structure of disordered materials that agree quantitatively with the available diffraction data and the measured density, provid-

ing that the data do not contain significant systematic errors. The fact that the method does not require any interatomic potential gives a great advantage compared to conventional simulation techniques for structural modeling of materials, where the existing interatomic model potentials cannot quantitatively reproduce the experimental facts.

Before one begins the actual RMC simulation it is convenient to run a hard-sphere Monte Carlo simulation to create a computer configuration that is consistent with the applied constraints. These constraints can be closest approach distance of two particles, maximum bond length, bond angles, and number of nearest neighbors. The constraints are usually determined from the experimental diffraction data or other experimental evidence such as NMR and Raman spectroscopic data. Thus, for the present glasses the constraints serve to produce initial configurations that are consistent with previous knowledge of the glasses, i.e., a three-dimensional network with three- and four-coordinated B in the case of the $(AgI)_x$-$(Ag_2O\text{-}2B_2O_3)_{1-x}$ glasses,[38] chains of interconnected PO_4 units for the $(AgI)_x$-$(AgPO_3)_{1-x}$ glasses,[39] and the presence of molecular MO_4^{2-} ions for the $(AgI)_{0.75}$-$(Ag_2MO_4)_{0.25}$ glasses ($M=$Mo, W). More details about the RMC simulations and the applied bonding constraints have previously been published in Refs. 30–33. However, it should be mentioned here that all glasses contained about 4000 atoms and periodic boundary conditions were used in cubic boxes. We also produced smaller configurations (containing approximately 600 atoms) to test the size dependence of the results. This showed that such a reduction of the box size did not have any significant effect on the results more than that the statistical errors increased due to the reduced number of mobile Ag^+ ions. Thus, the present structural models should be of sufficient size.

In addition to these previously used constraints, we also included a recently introduced[22] soft bond-valence sum constraint that minimized the valence difference $\Delta V=|V-1|$ of each Ag^+ ion during the fitting procedure to the diffraction data. For the calculation of the total bond-valence sum V we used Eqs. (1) and (2) where the parameter set in Eq. (2) was given by[40]

$$s_{\text{Ag-O}}=\exp\left[\frac{1.89\ \text{Å}-R_{\text{Ag-O}}}{0.33\ \text{Å}}\right], \tag{4a}$$

$$s_{\text{Ag-I}}=\exp\left[\frac{2.08\ \text{Å}-R_{\text{Ag-I}}}{0.53\ \text{Å}}\right]. \tag{4b}$$

The parameter set by Radaev, Fink, and Trömel[40] was chosen because it includes the influence of higher coordination shells, i.e., intermediate-range order in the glass, in contrast to other parameter sets that are generally influenced only by the short-range order, i.e., the bonds to the first coordination shell.

The valence difference ΔV was minimized in the RMC modeling in the same way as the deviations between the calculated and experimentally measured structure factors were minimized, i.e., by calculating

$$\chi_n^2(\text{valence})=\Delta V^2/\sigma^2(\text{valence}), \tag{5}$$

where σ(valence) is an input parameter that depends on the assumed ΔV. The value of χ_n^2(valence) was thereafter added to the contributions arising from deviations between the calculated and experimentally measured structure factors and deviations from the target coordination constraints (more details about these contributions are given in Refs. 35 and 36). A random atomic move is always accepted if $\chi_{n+1}^2(\text{total})<\chi_n^2(\text{total})$ and if $\chi_{n+1}^2(\text{total})>\chi_n^2(\text{total})$, the move is accepted with the probability $\exp[-(\chi_{n+1}^2-\chi_n^2)/2]$.

The effect of the additional bond-valence constraint on the structure will be shown in Sec. IV, however, it is worth noting here that it was not possible to fit the diffraction data with a strict constraint on the valence sum, i.e., a very low value of σ(valence), indicating that the individual Ag^+ ions in real glasses show some deviations from the empirical ideal valence sum of 1. This can be mostly traced back to the instantaneous nature of RMC structure models, as the RMC technique yields models for snapshots of the vibrating atomic ensemble rather than for the energy-minimized ideal structure.

IV. THE EFFECT OF THE BOND-VALENCE CONSTRAINT ON THE RMC RESULTS

The neutron and x-ray weighted structure factors $S(Q)$ of $AgPO_3$, AgI-$AgPO_3$, Ag_2O-$2B_2O_3$, $(AgI)_{0.6}$-$(Ag_2O\text{-}2B_2O_3)_{0.4}$, and $(AgI)_{0.75}$-$(Ag_2MoO_4)_{0.25}$ glasses obtained by RMC modeling are compared with those obtained experimentally in Figs. 2(a) and (b). The overall structure factors are well reproduced and, in particular, the computed x-ray data (which is most sensitive to the coordinations of the Ag^+ ions) are in excellent agreement with the experimental results. Thus, the good fits to the experimental $S(Q)$, in combination with the applied bond-valence constraint, should ensure that the RMC configurations contain realistic Ag^+ coordinations and the essential overall structural features of the investigated glasses.

Figure 3 shows how the bond-valence sum distribution of the Ag^+ ions is altered when the soft bond-valence constraint [given by Eq. (1)] is included in the RMC modeling. For all the three glasses shown in Fig. 3 the average value increases and the distribution gets narrower. The reason for the increased average value is mainly that the total average coordination number (Ag-O+Ag-I) increases slightly, and the reason for the reduced width is mostly due to the significantly reduced number of Ag^+ ions with exceptionally low bond-valence sums (see Fig. 3), i.e., low total coordination numbers (<2). Thus, the number of structural ''defects'' or unrealistic Ag coordinations have been reduced by the inclusion of the bond-valence constraint. The ratio of the Ag-O (or Ag-I) contribution to the total bond-valence sum is, however, not substantially changed by the constraint.

Although all the investigated glasses show broad distributions of total coordination numbers, their total average coordination numbers are remarkably similar and close to 3.5. For all the AgI-doped glasses most of the Ag^+ ions are co-

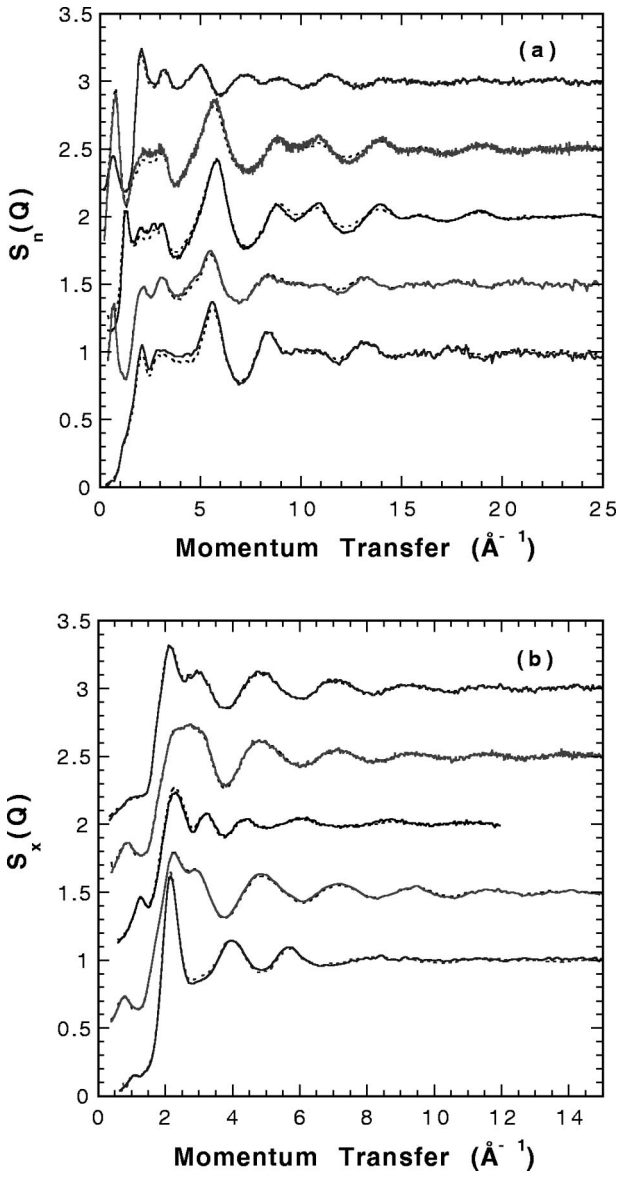

FIG. 2. Experimental neutron (a) and x-ray (b) structure factors (solid lines) and computed neutron weighted (a) and x-ray weighted (b) structure factors (dashed lines) for the RMC configurations of $AgPO_3$, AgI-$AgPO_3$, Ag_2O-$2B_2O_3$, $(AgI)_{0.6}$-$(Ag_2O$-$2B_2O_3)_{0.4}$, and $(AgI)_{0.75}$-$(Ag_2MoO_4)_{0.25}$. Consecutive curves are shifted by 0.5 for clarity.

ordinated to both O and I^-, but the ratio between the average Ag-I and Ag-O coordination numbers ($N_{\text{Ag-I}}/N_{\text{Ag-O}}$) increases with increasing AgI content in the glass. This means that the $(AgI)_{0.6}$-$(Ag_2O$-$2B_2O_3)_{0.4}$ glass has the highest $N_{\text{Ag-O}}=1.8$ and lowest $N_{\text{Ag-I}}=1.7$, whereas the $(AgI)_{0.75}$-$(Ag_2MoO_4)_{0.25}$ glass has the highest $N_{\text{Ag-I}}=2.5$ and lowest $N_{\text{Ag-O}}=1.0$. These findings are in agreement with EXAFS results, which have shown that the I^- ions of AgI-doped glasses tend to be coordinated to four Ag^+, on average.[41] In order to fulfill this criterion $N_{\text{Ag-I}}$ must increase with increasing AgI content. One should also note that Ag^+ ions in glasses of similar AgI content have similar distributions of coordination numbers.[33] Furthermore, it was found that differences in local average Ag^+ environments between glasses of different AgI contents seem to be closely related to their different ionic conductivities.[33]

V. RESULTS FROM THE RANDOM-WALK SIMULATION

The applicability of the chosen random-walk approach can be judged by comparing the resulting Ag^+ displacements and simulated ionic conductivities to experimental data in the literature. For the conversion from the displacement of the ''mobile'' ions (i.e., those within the bond-valence pathways) into the displacement for all Ag^+ of the structure model it was assumed that the displacement of the Ag^+ outside the path remains zero all the time. The resulting log-log plot of the root-mean-square (rms) displacement vs pseudotime steps averaged over all Ag^+ ions is shown in Fig. 4. A more realistic treatment including contributions of the thermal vibrations also for the Ag^+ outside the conduction pathways would alter the shape of the plots in Fig. 4 only for the first few time steps and cause a minor shift of all curves towards higher displacements. Our findings agree qualitatively with the results reported in Ref. 31.

For some of the systems Fig. 5 displays the variation of the slope of the displacement vs the time curve with the displacement (in this case averaged over the mobile ions only) as determined from higher-order polynomial fits to the respective curves of Fig. 4. The initial steep rise in all systems for low values of the rms displacement may be identified with unrestricted local vibrations of the mobile ions within the same local energy minimum. For crystalline AgI at 525 K [curve (b)] the slope distinctly decreases as the rms displacement approaches the distance between equilibrium sites (ca. 2 Å in α-AgI), since only a small fraction of the local jumps leads to a neighboring equilibrium site. On all larger length scales the crystalline system behaves homogeneously, so that the rms displacement increase becomes proportional to $t^{1/2}$ in accordance to the diffusion law. The exponent $\frac{1}{2}$ suggests that the connectivity of the conduction pathway network is considerably above the percolation threshold. For the amorphous systems $(d)-(i)$ the slope remains depressed below $\frac{1}{2}$ over an extended region. Although the detailed shape of the curves in Fig. 5 is biased by the chosen order of the polynomial fit, it may be concluded that the depression is more pronounced for glasses with low conductivities demonstrating the reduced connectivity of the pathway network in these systems. For the systems with the lowest conductivities the simulation period had to be extended to nearly 10^7 time steps in order to reach the long-time limit $\frac{1}{2}$ of the slope. For these systems the spatial extension of the region where the displacement increases slower than $t^{1/2}$ approaches the size of the simulated box, so that an influence of the periodic boundary conditions of the simulations cannot be ruled out.

A. Absolute conductivity

The simulated displacement versus pseudotime curves do not only appear plausible with respect to their shape. Figure 6 displays that atomic self-diffusion coefficient D

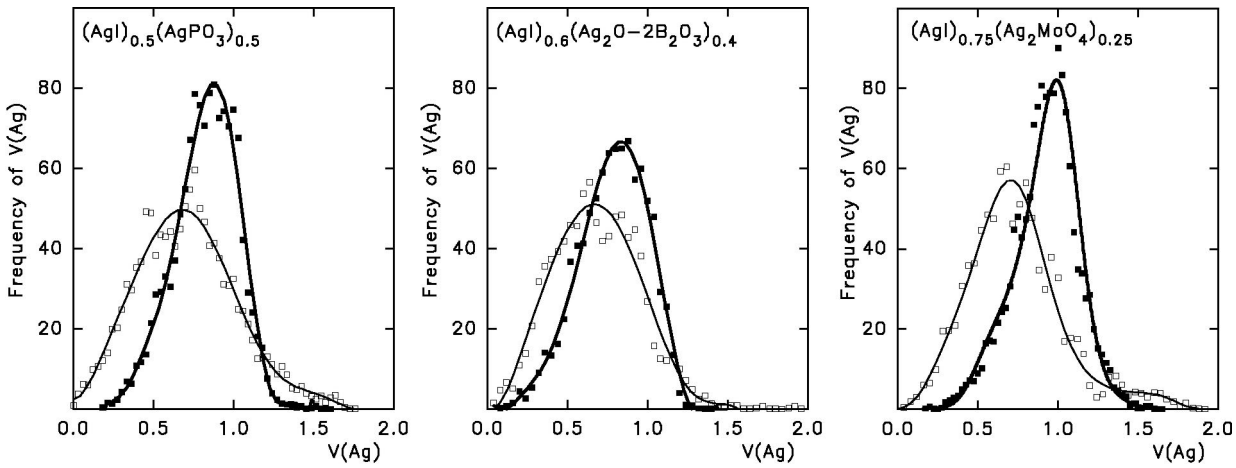

FIG. 3. Bond-valence sum distributions of the Ag^+ ions in AgI-$AgPO_3$, $(AgI)_{0.6}$-$(Ag_2O\text{-}2B_2O_3)_{0.4}$, and $(AgI)_{0.75}$-$(Ag_2MoO_4)_{0.25}$ before (open symbols) and after (filled symbols) the soft bond-valence constraint was included in the RMC modeling.

$=\langle R^2\rangle/6t$, as determined from the increase of the mean-square displacement $\langle R^2\rangle$ with time t in the linear long-time regime (which corresponds to the region with a slope of $\frac{1}{2}$ in Fig. 4), are closely correlated to the experimental conductivity $\sigma_{\rm exp}$ at the temperature T of the diffraction experiments on which the RMC structure models are based. The pseudotime scale of the simulations has been converted into real time by assuming that the Ag^+ hop around with a fixed velocity $\nu=\sqrt{3RT/M_{\rm Ag}}$, which leads to time steps of $0.7-1.1\times10^{-3}$ s depending on the temperature and the edge length of the volume elements in the respective model.

Thereby these simulations [like the correlation given in Eq. (3a)] can be used to predict the conductivity of a system from its structural model. It should however be noted that this correlation is nonlinear (as seen from the slope, which is >1 for the log-log plot in Fig. 6), due to the simplifications of our approach. In Fig. 7 the simulated diffusion constants are converted into calculated conductivities $\sigma_{\rm calc}$ by means of the Nernst-Einstein equation

$$\sigma T = D\cdot c_{\rm Ag}\cdot\frac{z^2F^2}{R}. \tag{6}$$

Despite the crude simplifications of the approach the simulations reproduce the correct order of magnitude for conductivities of the fast ion-conducting glasses [systems $(c)-(e)$ and $(k)-(l)$] but systematically overestimate the conductivities for glasses with low conductivities and underestimate the conductivities in the crystalline superionic α-AgI.

Thus the basic assumption of a free motion within bond-valence pathways may be an admissible simplification in the most interesting cases of glasses with high ionic conductivities. For glasses with conductivities below approximately $10^{-5}\,\Omega\,{\rm cm}^{-1}$ it might be more appropriate to describe the motion even within the pathways as impeded by (bond-valence mismatch) barriers. The transport mechanism for these systems with low conductivities thus would bear some similarity to the weak electrolyte theory[42] that had been proposed earlier to apply to all ion-conducting glasses. These

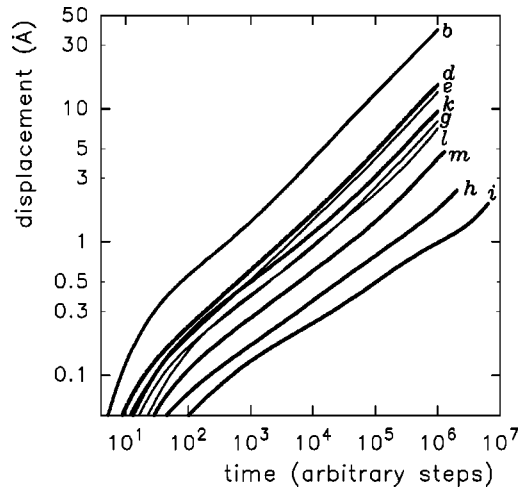

FIG. 4. Variation of the Ag displacement vs simulation time steps for all Ag^+ in the system. The nomenclature of the systems is identical to that in Fig. 1.

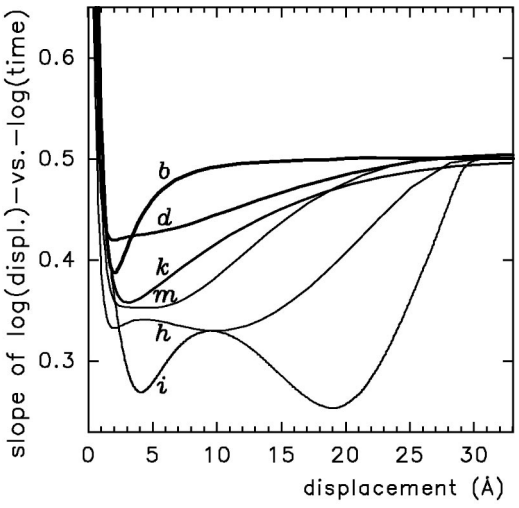

FIG. 5. Variation of the slope of the rms displacement vs number of time steps as a function of displacement for the ''mobile Ag^+.''

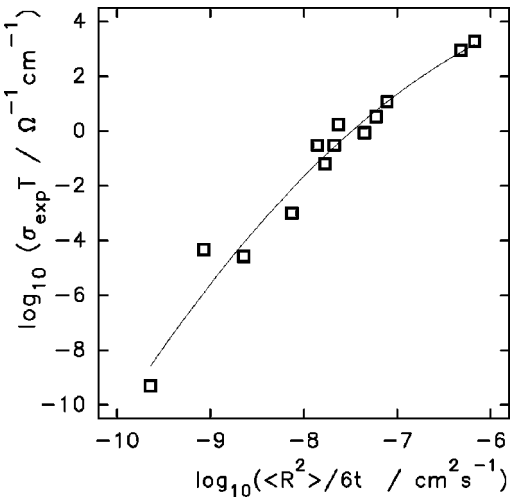

FIG. 6. Correlation between the atomic self-diffusion constant $\langle R^2\rangle/6t$ for all Ag^+ in the random-walk simulations and the experimental conductivities σ_{exp}.

migration barriers could be incorporated in a more refined Monte-Carlo-like version of our simulations, where the probability of hops is related to some (steep) function of the valence mismatches at both the starting position and at the target site instead of the simplistic step function we used in this work. Furthermore, the underestimation of the conductivity for the case of superionic α-AgI might indicate that the treatment of the transport process as a motion of a single particle in an otherwise frozen environment is no longer appropriate. Most likely, one has to account for the unusually large anion displacements in α-AgI and for the possibility of correlated cation jumps.

The value of the bond-valence mismatch threshold ΔV may be thought of as representing a migration barrier that a mobile Ag^+ with an average kinetic energy is able to cross with a certain probability. However, although the choice of the bond-valence mismatch threshold $\Delta V = 0.05$ in this study is to some extent arbitrary, a slight variation of the threshold value would affect the simulated conductivities only marginally. Increasing the valence mismatch threshold to $\Delta V = 0.1$ raises the simulated conductivity of AgI at 525 K by a factor of ~ 2 only. For the glass systems the relative change of F as a function of the choice of ΔV is even smaller and therefore the simulated diffusion coefficient should be even less dependent on the choice of ΔV.

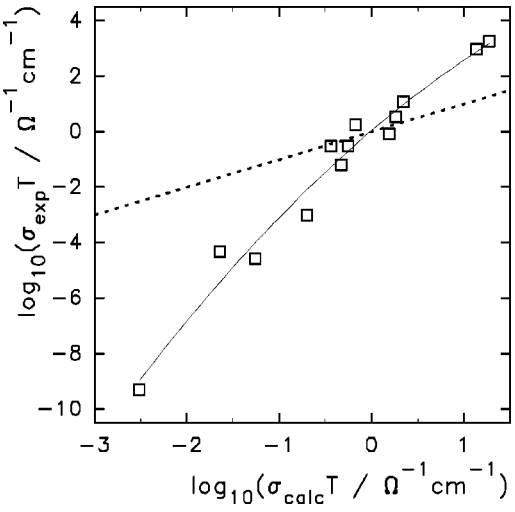

FIG. 7. Correlation between the conductivities σ_{calc} from the random-walk simulations and the experimental conductivities σ_{exp}. The dotted line indicates the ideal case $\sigma_{calc} = \sigma_{exp}$.

B. Role of Ag^+ coordination

For silver iodide silver oxyacid glasses the relative contribution of silver ions with different types of coordinations to the ionic conductivity has been a matter of intense discussion. It has, for instance, been proposed that the mobile silver ions are almost entirely located in small clusters of AgI and that the remaining silver ions are immobilized by the oxygens of the host glass.[43] A different model for ion conduction had earlier been proposed by Greaves,[44] who suggested from EXAFS experiments that the mobile cations are not homogeneously distributed in the glass but rather confined to channellike regions, which then should also form pathways for ion transport. A corresponding model can be constructed in the case of AgI-doped glasses assuming that the salt ions are preferably located in similar pathways running through the glassy matrix. In contrast to the model proposed by Rousselot *et al.*,[43] Ag^+ ions with a mixed oxygen/iodine coordination are typically the dominant Ag^+ species according to RMC structure models.[30,31,33] Thus it may be assumed that these Ag^+ should significantly contribute to the ionic conductivity.[22] Our random-walk simulations provide a simple tool to test the supposition that oxygen coordinated Ag^+ are immobile in the glassy ionic conductors and in principle even to quantify the effect of different types of coordinations.

Therefore we performed simulations of the Ag^+ transport within the bond-valence pathways of RMC models of several glasses under various limiting conditions with regard to the type of coordinating anions. This was achieved by defining that only sites for which the Ag-O contribution to the total bond-valence sum remains below a given threshold value can be ''accessible'' for the mobile Ag^+. Figure 8 displays the variation of the simulated displacement versus pseudotime for three of the glass systems under various assumptions on the involvement of differently coordinated sites in the ion transport process. While the fundamental effect is the same in all the investigated glasses the reduction of the ion mobility by the exclusion of predominantly oxide coordinated sites is naturally most pronounced in glasses with a high contribution from Ag-O coordinations, such as in the $(AgI)_{0.6}$-$(Ag_2O\text{-}2B_2O_3)_{0.4}$ glass (see Sec. IV). Within the modeled time scale an increase in the displacement proportional to t^γ, with $\gamma = \frac{1}{2}$ (as expected for a network with a connectivity considerably above the percolation threshold) is observed only if the maximum contribution from Ag-O bonds to the Ag valence sum in the pathway is unrestricted. More and more rigorous restrictions of the maximum allowed relative contribution of Ag-O bonds to the valence sum result in a reduced slope γ in the log-log plot. Under the

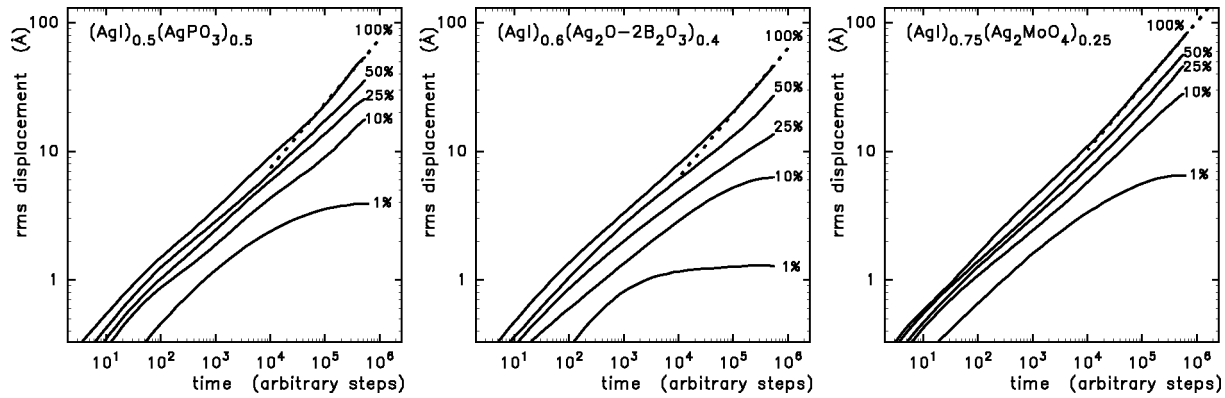

FIG. 8. Simulated rms displacements vs pseudo time steps for mobile Ag^+ in the bond-valence pathway models of the glasses $(AgI)_{0.5}(AgPO_3)_{0.5}$, $(AgI)_{0.6}(Ag_2O\text{-}2B_2O_3)_{0.4}$ and $(AgI)_{0.75}\text{-}(Ag2MoO_4)_{0.25}$. Five different limiting conditions for sites within the conduction pathway were used regarding the maximum allowed contribution of Ag-O bonds to the total Ag valence sum (expressed as percentages). Broken lines indicate the slope $\frac{1}{2}$ to be expected as the long-time limit for networks significantly above the percolation threshold.

extreme condition that only purely iodine-coordinated sites may contribute to the ion conduction, Ag^+ motion would remain restricted to local hops in all three glasses since no long-range conduction pathway exist.

C. Correlated forward-backward hopping

The interpretation of conductivity spectra of ion-conducting glasses generally shows that the hopping conductivity $\sigma_{\rm hop}$ (after eliminating vibrational contributions) depends on the frequency ω according to a power law of the type

$$\sigma_{\rm hop}(\omega)-\sigma(0)=A\left(1+\frac{1}{\omega t_1}\right)^{-p_A}+B\left(1+\frac{1}{\omega t_1}\right)^{-p_B}. \tag{7}$$

The first right-hand-side term with an exponent $p_A<1$ (typically ca. 0.7) is mostly explained in terms of the jump relaxation model[45,46] as a consequence of the interplay between backward hops and relaxations of the environment forced by the mismatch at the target site. The second often dominating term with an exponent $p_B>1$ would then correspond to a backward hopping that is faster than the site relaxation. In the ''unified site relaxation model''[47] this is taken as an indication for the existence of a second type of ''bad'' target sites (from which the moving ion necessarily hops back to its previous position after some time).

In our simple approach all the ions of the model, except for the moving Ag^+ ion, remain fixed. Thus there is no relaxation of the environment and any preference of correlated forward-backward hops can only be due to the second type. However, also these fast forward-backward hops are difficult to simulate using our method. This is partly because our ionic hops are only accepted if the target sites fulfill the bond-valence criterion and furthermore the hops are much too short for the Ag^+ ions to be able to reach new possible equilibrium sites. Thus, to really elucidate the high-frequency conduction mechanism a much more sophisticated method has to be used. However, since the direction of motion during our simulation is chosen randomly among the 26 adjacent for every individual hop, the requirement that only sites that fulfill the bond-valence criterion are accessible target sites drastically reduces the number of potential target sites. This by itself gives rise to a statistical preference of correlated forward-backward hops, which are clearly seen in Fig. 9 for the motion of an Ag^+ ion through the bond-valence pathways in the RMC model of glassy $AgPO_3$. The figure illustrates the oscillatory nature of the simulated motion also on relatively long-time scales. Although the starting point of the random walk for the arbitrarily selected Ag^+ is located within the continuous pathway, the trajectory includes a huge number of forward-backward hops between pairs of neighboring sites (jump distance <2 Å) as well as numerous forward-backward motions between the starting position and another position at a distance of about 10 Å. In this example it takes about 250 000 trials ($\approx$22 ns) until the Ag^+ ion finds its way through a bottle neck out of this region of the pathway and—after crossing several other local loops of the pathway—the trajectory again leads back to the same region about 80 000 time steps later. Thus, although this approach is very crude it shows the potential of the method to gain some insight into also the frequency-dependent conductivity. Similar statistical arguments can be given to partly explain the high-frequency conductivity in real systems, since with a large number of energetically unfavorable sites around each Ag^+ ion one would expect, from a pure statistical consideration, a high probability of forward-backward hops. Thus, although the present results are not able to quantitatively reproduce the frequency behavior of the conductivity, one can gain some qualitative understanding of why the ionic mobility is larger on a local length scale than on a more macroscopic length scale and why the ionic conductivity increases with increasing applied frequency.

VI. CONCLUDING REMARKS

As demonstrated in this work the reverse Monte Carlo modeling method and the bond-valence approach are

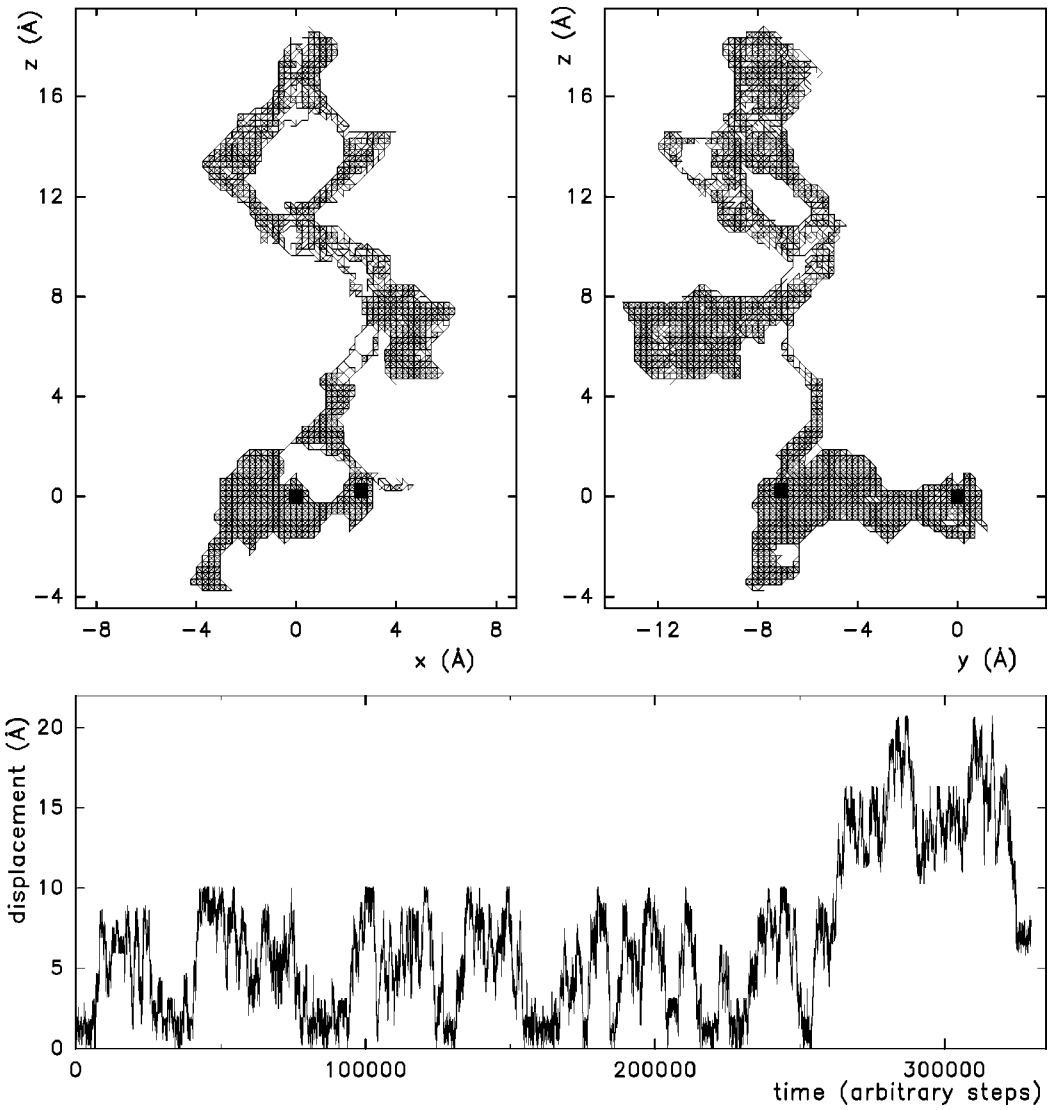

FIG. 9. Trajectory for the motion of an Ag^+ ion in glassy $AgPO_3$ [system (*n*)] over 330 000 simulation time steps=82 282 actual hops projected on the *xz* and *yz* planes (top row). Starting position at (0, 0, 0) and the final position are marked by ■■ Bottom: Variation of the displacement from the starting point versus the number of time steps for the same Ag^+ ion.

complementary tools for investigating the relation between microscopic structure and macroscopic properties. The combination of the two methods gives a unique possibility for elucidating the ion-conduction mechanism and for finding the most important structural properties for high conductivity. In this approach we are using bond-valence constraints that are incorporated in the RMC-produced structural models in order to obtain physically more sensible local environments of the mobile ions. Thereafter, the bond-valence approach is again applied on these refined structural models to investigate the ion transport in fast ion-conducting glasses. The combination of these two tools appears quite natural because both the RMC configurations and the determination of bond-valence parameters are directly based on experimental diffraction data.

Despite its simplicity, the description of Ag^+ motion as a random walk within bond-valence pathways can be effectively used to predict the ionic conductivity from a structural model. Moreover, the difference between the close reproduction of experimental conductivity data in the case of superionic glasses and systematic deviations both for crystalline superionic conductors and glasses with low conductivities may help to understand the peculiarities of the respective transport mechanisms.

The static nature of RMC-produced structural models and thus also of the pathway models might lead to the misconception that temperature has no effect on the simulated diffusion. However, this is not the case since different temperatures means different densities and different diffraction data, which in turn lead to different RMC structure models. This was clearly observed for crystalline α-AgI, where the structural model based on diffraction data taken at 740 K shows a higher volume fraction of bond-valence pathways than the corresponding model based on diffraction data taken at 525 K. A higher volume fraction of bond-valence pathways generally promotes the conductivity by a higher cross section of pathways, a higher connectivity of the pathway network, and by a higher fraction of ''mobile'' ions. All these factors con-

tribute to the differences in conductivity between the ion-conducting solids studied here.

ACKNOWLEDGMENTS

We are grateful to Dr. R. L. McGreevy and Dr. V. M. Nield for the RMC configurations of α-AgI at 525 and 740 K as well as the previous RMC configurations of the silver phosphate glasses. We are also indebted to Professor L. Börjesson for experimental neutron-diffraction data on silver borate glasses. Financial support to J.S. from the Swedish Natural Science Research Council and to St.A. from the Deutsche Forschungsgemeinschaft is gratefully acknowledged.

[1] P. A. V. Johnson, A. C. Wright, and R. N. Sinclair, J. Non-Cryst. Solids **50**, 281 (1982).
[2] J. Swenson and L. Börjesson, Phys. Rev. B **55**, 11 138 (1997).
[3] L. E. Busse, Phys. Rev. B **29**, 3639 (1984).
[4] P. H. Gaskell and D. J. Wallis, Phys. Rev. Lett. **76**, 66 (1996).
[5] M. F. David and A. J. Leadbetter, Philos. Mag. B **44**, 509 (1981).
[6] A. Uhlherr and S. R. Elliott, J. Phys.: Condens. Matter **6**, L99 (1994); Philos. Mag. B **71**, 611 (1995).
[7] P. S. Salmon, Proc. R. Soc. London, Ser. A **445**, 351 (1994).
[8] D. L. Price, S. C. Moss, R. Reijers, M. L. Saboungi, and S. Susman, J. Phys.: Condens. Matter **1**, 1005 (1989).
[9] S. R. Elliott, Phys. Rev. Lett. **67**, 711 (1991); J. Phys.: Condens. Matter **4**, 7661 (1992).
[10] J. Swenson and L. Börjesson, J. Non-Cryst. Solids **223**, 223 (1998).
[11] H. Iyetomi and P. Vashishta, Phys. Rev. B **47**, 3063 (1993).
[12] A. Nakano, R. K. Kalia, and P. Vashishta, J. Non-Cryst. Solids **171**, 157 (1994).
[13] R. L. McGreevy and L. Pusztai, Mol. Simul. **1**, 359 (1988).
[14] D. A. Keen and R. L. McGreevy, Nature (London) **344**, 423 (1990).
[15] D. A. Keen, Phase Transitions **61**, 109 (1997).
[16] K. Waltersson, Acta Crystallogr., Sect. A: Cryst. Phys., Diffr., Theor. Gen. Crystallogr. **34**, 901 (1978).
[17] I. D. Brown, Acta Crystallogr., Sect. B: Struct. Sci. **53**, 381 (1997); **B48**, 553 (1992).
[18] St. Adams, Solid State Ionics **136/137**, 1351 (2000).
[19] N. E. Brese and M. O'Keeffe, Acta Crystallogr., Sect. B: Struct. Sci. **B47**, 192 (1991).
[20] I. D. Brown, in *Structure and Bonding in Crystals*, edited by M. O'Keeffe and A. Navrotsky (Academic, New York, 1981), Vol. II, pp. 1–30.
[21] St. Adams, Acta Crystallogr, Sect. B: Struct. Sci. **B57**, 278 (2001).
[22] St. Adams and J. Swenson, Phys. Rev. B **84**, 4144 (2000); Phys. Rev. B **63**, 054201 (2001).
[23] J. D. Garrett, J. E. Greedan, R. Faggiani, S. Carbotte, and I. D. Brown, J. Solid State Chem. **42**, 183 (1982).
[24] R. Withers, S. Schmid, and J. G. Thompson, Prog. Solid State Chem. **26**, 1 (1998).
[25] St. Adams and J. Maier, Solid State Ionics **105**, 67 (1998).
[26] St. Adams, W. F. Kuhs, and D. Wilmers, Z. Kristallogr. Suppl. **16**, 87 (1999).
[27] St. Adams and A. Preusser, Acta Crystallogr., Sect. C: Cryst. Struct. Commun. **55**, 1741 (1999).
[28] J.-S. Lee, St. Adams, and J. Maier, J. Phys. Chem. Solids **61**, 1607 (2000).
[29] St. Adams, J. Solid State Chem. **149**, 75 (2000).
[30] J. Swenson, L. Börjesson, R. L. McGreevy, and W. S. Howells, Phys. Rev. B **55**, 11 236 (1997).
[31] J. Wicks, L. Börjesson, R. L. McGreevy, W. S. Howells, and G. Bushnell-Wye, Phys. Rev. Lett. **74**, 726 (1995).
[32] J. Swenson, R. L. McGreevy, L. Börjesson, J. D. Wicks, and W. S. Howells, J. Phys.: Condens. Matter **8**, 3545 (1996).
[33] J. Swenson, R. L. McGreevy, L. Börjesson, and J. D. Wicks, Solid State Ionics **105**, 55 (1998).
[34] R. J. Cava, F. Reidinger, and B. J. Wuensch, Solid State Commun. **24**, 411 (1977).
[35] R. L. McGreevy and M. A. Howe, Annu. Rev. Mater. Sci. **22**, 217 (1992).
[36] R. L. McGreevy, Nucl. Instrum. Methods Phys. Res. A **354**, 1 (1995).
[37] N. Metropolis, A. W. Rosenbluth, M. N. Rosenbluth, A. H. Teller, and E. Teller, J. Phys. Chem. **21**, 1087 (1953).
[38] S. A. Feller, W. J. Dell, and P. J. Bray, J. Non-Cryst. Solids **51**, 21 (1982).
[39] R. K. Brow, C. C. Phifer, G. L. Turner, and R. J. Kirkpatrick, J. Am. Ceram. Soc. **74**, 1287 (1991).
[40] S. F. Radaev, L. Fink, and M. Trömel, Z. Kristallogr. Suppl. **8**, 628 (1994); M. Trömel (private communication).
[41] F. Rocca, G. Dalba, P. Fornasini, and A. Tomasi, Solid State Ionics **53–56**, 1253 (1992).
[42] D. Ravaine and L. Souquet, Phys. Chem. Glasses **18**, 27 (1977).
[43] C. Rousselot, J. P. Malugani, R. Mercier, M. Tachez, P. Chieux, A. J. Pappin, and M. D. Ingram, Solid State Ionics **78**, 211 (1995).
[44] G. N. Greaves, J. Non-Cryst. Solids **71**, 203 (1985).
[45] K. Funke, Prog. Solid State Chem. **22**, 11 (1993).
[46] K. Funke, J. Non-Cryst. Solids **172–174**, 215 (1994).
[47] A. Bunde, K. Funke, and M. D. Ingram, Solid State Ionics **86–88**, 1311 (1996).